



Article

Biosynthesis of Silver Nanoparticles from Fermented Bush Tea (*Athrixia phylicoides* DC) Leaf Extract and Evaluation of Their Antioxidant and Antimicrobial Properties

Mpho Edward Mashau ¹, Theshano Mamagau ¹, Kgethego Foforane ¹, Bono Nethathe ¹,
Maanea Lonja Ramphinwa ² and Fhatuwani Nixwell Mudau ^{3,*}

¹ Department of Food Science and Technology, Faculty of Science, Engineering and Agriculture, University of Venda, Thohoyandou 0950, South Africa; mpho.mashau@univen.ac.za (M.E.M.); mamagautheshano@gmail.com (T.M.); foforanegethego@gmail.com (K.F.); bono.nethathe@univen.ac.za (B.N.)

² Department of Plant and Soil Sciences, Faculty of Science, Engineering and Agriculture, University of Venda, Thohoyandou 0950, South Africa; maanea.ramphinwa@univen.ac.za

³ School of Agricultural, Earth and Environmental Sciences, University of Kwa-Zulu Natal, Pietermaritzburg 033, South Africa

* Correspondence: mudauf@ukzn.ac.za

Abstract: Green synthesis is a promising strategy for producing eco-friendly, non-toxic, and less expensive metallic nanoparticles from plants and microorganisms. This research synthesized silver nanoparticles (AgNPs) from fermented leaf extract of bush tea (*Athrixia phylicoides* DC). The physicochemical characterization of AgNPs was conducted by UV-vis spectroscopy, Fourier Transform Infrared Spectrometry (FTIR), and Differential Scanning Calorimetry (DSC). In addition, the total phenolic and flavonoid contents, antioxidant and antimicrobial activities of AgNPs were evaluated. The results indicated the successful formation of AgNPs by a visual change of color in fermented bush tea leaf extract from black to brown and in unfermented bush tea leaf crude extract from dark brown to light brown. The UV-vis spectrum of the reaction of the mixture of synthesized AgNPs with unfermented and fermented bush tea showed maximum absorbance at 457 nm and 450 nm, which confirmed the formation of AgNPs. FTIR revealed the functional groups of a leaf extract from bush tea that contributed to the reduction and capping process. The thermal properties suggest that low thermal stable compounds contributed to the reduction of Ag⁺ to Ag⁰ in the phyto compounds found in the extract. The total phenolic content was higher in fermented AgNPs (290.44 mg/g GAE) compared to unfermented AgNPs (171.34 mg/g GAE). On the other hand, the total flavonoid content was higher in unfermented AgNPs (17.87 mg/g CE) than in fermented AgNPs (9.98 mg/g CE). Regarding antioxidant activity values, unfermented AgNPs had the highest FRAP (535.30 TE/mL) and 47.58% for DPPH. Fermented AgNPs had more antimicrobial activity than unfermented AgNPs. The results show that bush tea leaf extract can be used in different industries such as food, cosmetics, and biomedical.

Keywords: bush tea; nanoparticles; green synthesis; antioxidant properties; antimicrobial activity



Citation: Mashau, M.E.; Mamagau, T.; Foforane, K.; Nethathe, B.; Ramphinwa, M.L.; Mudau, F.N. Biosynthesis of Silver Nanoparticles from Fermented Bush Tea (*Athrixia phylicoides* DC) Leaf Extract and Evaluation of Their Antioxidant and Antimicrobial Properties. *Fermentation* **2023**, *9*, 648. <https://doi.org/10.3390/fermentation9070648>

Academic Editor: Chunwang Dong

Received: 1 June 2023

Revised: 6 July 2023

Accepted: 7 July 2023

Published: 10 July 2023



Copyright: © 2023 by the authors. Licensee MDPI, Basel, Switzerland. This article is an open access article distributed under the terms and conditions of the Creative Commons Attribution (CC BY) license (<https://creativecommons.org/licenses/by/4.0/>).

1. Introduction

Nanotechnology is one of the most excellent and fascinating research areas of the twentieth century, rapidly developing and impacting a wide range of human life [1]. Due to the increasing number of toxic substances in the environment, the development of new materials for synthesizing metal nanoparticles has become a daunting task. The primary challenge is to use environmentally friendly materials to generate metal nanoparticles [2]. In producing silver nanoparticles of various sizes and shapes, several chemical and physical processes, such as ultraviolet irradiation, microwave irradiation, chemical reduction,

photochemical method, electron irradiation, and sono-electrochemical method, have been used [3,4]. However, there are evident drawbacks to using these strategies, which have led to a decrease in their use. The production of volatile vapors and carbon dioxide, which have remarkably detrimental effects on both the environment and people, as well as the use of harsh conditions such as heat, pressure, and pH during various steps of the synthesis of nanoparticles, are among these drawbacks. Organic solvents used in nanoparticle synthesis also have reproductive and neurobehavioral effects [5–7].

Metal nanoparticles such as silver (Ag), gold (Au), platinum (Pt), and palladium (Pd) are very easy to synthesize and are widely used for numerous applications [8]. However, silver nanoparticles (AgNPs) are currently the most studied nanoparticles due to their unique physical, chemical, and biological characteristics, lack of toxicity, and exhibit better antimicrobial activity [9,10]. AgNPs are used as anti-bacterial, anti-fungal, anti-inflammatory agents, antiviral, antiangiogenic, and antiplatelet activities [11,12]. Moreover, AgNPs have shown great potential for active food packaging applications in the health and food industries [13]. Unfortunately, some toxic chemical species can be absorbed by nanoparticles during chemical synthesis, which can adversely affect the application [14]. This can be easily eliminated using a green process; therefore, green processes of nanoparticle synthesis should be developed. Green synthesis is an environmentally friendly alternative to chemical synthesis [15] and can be developed on a large scale, more advanced than chemical synthesis [16,17]. The ability of plants to synthesize nanoparticles in non-aseptic circumstances makes them an attractive option. The use of plants and plant extracts in green synthesis has gained popularity due to rapid growth, single-step technique, cost-effective procedures, non-pathogenicity, and environmental friendliness for nanoparticle synthesis [18].

Biology and medicine have used AgNPs as antimicrobial substances because they have strong biocidal effects on microorganisms [19]. They have been used for many years to prevent and cure ailments and infections. Recently, applications such as food containers, clothing, coatings, and wound dressings have used AgNPs [20]. The US Food and Drug Administration has approved the application of some AgNPs. Nanoparticles have already been utilized in various applications, and various studies have been conducted on generating nanoparticles using plant extract. The biosynthesis of AgNPs using plants is the preferred method due to its fast, easy, eco-friendly, nonpathogenic, cost-effective, conservative convention and the introduction of a solitary advance strategy for biosynthetic procedures [21]. This includes the synthesis of AgNPs using a leaf extract of green tea [17], *Aristolochia bracteolata* lam [19], *Enicostemma axillare* [22], *Tribulus terrestris* [23] and *Cocos nucifera* [24].

Athrixia phyllicoides, also known as “bush tea,” is a herbal native shrub-like plant in different parts of South Africa [25,26]. The plant is distinguished by tiny dark green leaves and small pinkish/purple flowers with a yellow center [26]. The flowering season runs from March to May, but flowers can develop anytime throughout the year [27]. Bush tea has high levels of polyphenols, tannins, and flavonoids, and these compounds are beneficial for various health conditions [28,29]. Moreover, its leaves contain 5-hydroxy-6,7,3',4',5'-hexamethoxy flavon3-ol flavonoids, which are considered responsible for plant bioactivity. In South Africa, people have used this herb for centuries to treat various ailments, such as cuts and infections, and to cleanse and as a foam bath [27].

Currently, reports on the green synthesis of AgNPs using bush tea leaf extract are minimal. This is the first study in which the extract of bush tea leaf was used to produce green synthesized AgNPs. However, Kaningini et al. [30] synthesized and characterized zinc oxide nanoparticles from bush tea leaf extract. Therefore, the current study biosynthesized AgNPs using extracts from fermented leaves of bush tea and evaluated their antioxidant and antimicrobial properties. It is important to investigate the utilization of fresh bush tea leaf extract to synthesize AgNPs since it has the potential to be used as a wound treatment that can be packaged as infusions or fluids.

2. Materials and Methods

2.1. Plant Materials and Chemicals

Fresh bush tea leaves were harvested from an experimental farm at the University of Venda, Thohoyandou, Limpopo province, South Africa. First, distilled water was used to rinse the harvested leaves to remove any dust particles and dirt; then, the leaves were air dried to complete dryness. No heat was used during the drying process to avoid destroying heat-sensitive phyto compounds. The dried leaves were ground into a fine powder using a Retsh ZM 200 ultracentrifugal miller. Half of the powdered leaves were allowed to ferment in a dark place at room temperature for seven months, and the rest of the powdered leaves of bush tea (unfermented) were stored in an airtight container until use. The powdered unfermented leaf extract of bush tea was used as a control. Silver nitrate (AgNO_3) was purchased from Rochelle Chemicals (Midrand, South Africa).

2.2. Preparation of Bush Tea Leaf Extract

The method of Ayinde et al. [31] was used to prepare the fermented and unfermented bush tea leaf extract with few modifications. About 25 g of bush tea leaf powder was weighed in a 500 mL beaker with 100 mL of distilled water. The solution was kept in the water bath for 20 min at 80 °C. After 20 min, the solution was allowed to cool before filtering through Whatman paper. Both extracts were stored in the refrigerator (4 °C) until further use.

2.3. Green Synthesis of Silver Nanoparticles

The AgNPs solution was obtained using microwave-assisted synthesis. In a 250 mL Erlenmeyer flask, 12 mL of bush tea leaf extract was reacted with 100 mL of 1 mM AgNO_3 solution to reduce Ag^+ to Ag^0 . The mixture was then microwaved for 30 s in a 2450 MHz frequency turntable domestic microwave oven (Ottimo, 20 L) set to medium power. This procedure was carried out for both fermented and unfermented bush tea leaf extract. The color change of the solution was visually observed. All analyses were duplicated to ensure the reliability of the results.

2.4. Characterization of Green Synthesized Silver Nanoparticles

Visual observation: AgNPs formed in fermented bush tea were visually observed when the color changed from black to dark brown, while the unfermented tea changed from dark brown to light brown.

A UV-vis spectrophotometer (SPECTROstar Nano/BGM LABTECH, Midrand, South Africa) was used to determine the optical properties of AgNPs. After adding AgNO_3 to the crude plant extract, the solutions were microwaved for 30 s, and the spectra were taken for two solutions between 290 and 1000 nm. Distilled water was used as a blank sample [32].

FTIR spectroscopy (Spectrum TwoTM FT-IR Spectrometer; PerkinElmer, Waltham, MA, USA) was used to study the function and composition of AgNPs that were produced [33]. The crude plant samples (fermented and unfermented bush tea leaf extract) were mixed with 1 mM AgNO_3 and microwaved. Solutions were characterized in the range 3500–500 cm^{-1} . The modes of these vibrations were assigned to identify different functional groups available in the leaf extract of bush tea.

Thermal measurements: A differential scanning calorimeter (DSC 4000, Perkin-Elmer, Shelton, CT, USA) was used to measure the thermal characteristics of the AgNPs, where indium was used for calibration. AgNPs from fermented and unfermented crude extracts between 5 mg and 6 mg were weighed in an aluminum pan, while an empty pan was used as a reference sample. The samples were in triplicate and were both heated under the flow of 50 mL per minute of synthetic air from room temperature to 100 °C at heating rates of 10 °C per minute.

2.5. Antioxidant Properties of Green Synthesized Silver Nanoparticles

2.5.1. Determination of the Total Phenolic Content

The Folin–Ciocalteu assay was used to evaluate the total phenolic content of bush tea leaf extract as well as the reaction solution generated from the leaf extract of bush tea [34]. Briefly, 0.5 mL of bush tea leaf extract, fermented and unfermented AgNPs reaction solution was added to the test tubes individually. The Folin–Ciocalteu reagent was individually added to 0.5 mL of the bush tea leaf extract, fermented, and unfermented reaction solution. The mixtures were kept for 5 min, and then 2 mL of 7.5% sodium carbonate was added and allowed to incubate for 45 min in the dark with intermittent shaking. The development of blue color was noticed after incubation. Spectrophotometry (Biowave II, 80-3003-75, Biochrom Ltd., Cambridge, UK) at 725 nm was used to determine total phenolic content, expressed as gallic acid equivalent (GAE) per gram of the sample.

2.5.2. Determination of Total Flavonoid Content

The aluminum chloride colorimetric method was used to measure the total flavonoid content of bush tea leaf extract, fermented and unfermented AgNPs from the leaf extract of bush tea [34]. Approximately 0.3 mL of bush tea leaf extract, fermented and unfermented AgNPs reaction solution was added into different 10 mL test tubes, 3.4 mL of 30% methanol was also added in each test tube, 0.15 mL of 0.5 M NaNO₂ was added to the test tubes, and 0.15 mL of 0.3 M AlCl₃·6H₂O was also added. Then, 1 mL of 1 M NaOH was added after 5 min. The absorbance against the reagent blank was measured at 506 nm using a UV-visible spectrophotometer. A catechin standard solution was used to make the total flavonoids standard curve. The results were expressed as mg equivalent catechins per g of sample.

2.5.3. DPPH Radical Scavenging Assay

The free radical scavenging capacity of the AgNPs reaction solution was measured by the DPPH assay using the modified method of Souza et al. [35]. About 2 mL of fermented and unfermented AgNPs reaction solution was separately added to 2 mL of 0.1 mM DPPH in 10 mL test tubes. The mixture in both test tubes was shaken vigorously. After the mixtures were kept for 30 min at room temperature, a UV-visible spectrophotometer was used to read the absorbance at 517 nm. The DPPH scavenging effects were calculated using the equation: % DPPH Radical Scavenging Activity = $(A_c - A_s) / A_c \times 100\%$. A_c = Control absorbance of methanol and DPPH radical, A_s = Sample absorbance of nanoparticles and DPPH radical.

2.5.4. Ferric Reducing Power Assay

The method of Lin et al. [36], with few modifications, was used to determine the reducing power of AgNPs. Approximately 0.5 mL of fermented AgNPs and unfermented AgNPs reaction solution was poured into different test tubes. In each test tube, 2.5 mL of potassium ferricyanide (1%) and 2.5 mL of phosphate buffer (0.2 M, pH 6.6) were added, and then the supernatants were incubated at 50 °C for 20 min. Approximately 2.5 mL of trichloroacetic acid (10%) was added to the supernatants before centrifuging for 10 min at 3000 rpm. About 2.5 mL of distilled water was added to the supernatant solution (2.5 mL) before mixing with 0.5 mL FeCl₃ (0.01%); a UV-visible spectrophotometer measured the absorbance at 700 nm.

2.6. Antimicrobial Activity of Green Synthesized Silver Nanoparticles

Three bacterial strains, Gram-positive *Bacillus cereus* American Type Culture Collection (ATCC) 10876 (*B. cereus*), Gram-positive *Staphylococcus epidermidis* ATCC 12228 (*S. epidermidis*), Gram-negative *Escherichia coli* ATCC 25922 (*E. coli*), and one fungus *Candida albicans* ATCC 10231 (*C. albicans*) were used for the antimicrobial activity of green synthesized fermented and unfermented AgNPs. Bacteria and fungi were obtained from Davies Diagnostic, Randburg, South Africa. The streaking method was used to culture all bacteria

strains on Mueller Hinton agar (MHA) (Merck, Germany) and incubated at 37 °C for 24 h. The susceptibility test was performed with two methods for comparison.

2.6.1. Agar Well Diffusion Method

The antimicrobial effectiveness of the green synthesized AgNPs was tested against *E. coli*, *S. epidermidis*, *B. cereus*, and *C. albicans*. The freshly cultured pure colonies were carefully spread on Mueller-Hinton agar (MHA) using a sterile cotton swab. A sterile pipette tip (7 mm in diameter) was used to drill four holes in each Petri dish to make the wells. The wells were loaded with 10 µL of the crude extracts, AgNO₃ solution (10 mM), distilled water (as negative control), and AgNPs separately. The Petri dishes were incubated. After 24 h of incubation at 37 °C, a clear zone around the colonies was observed, and the results were tabulated. This procedure was used for fermented and unfermented AgNPs solution obtained from bush tea leaf extract.

2.6.2. Disk Diffusion Method

The Kirby–Bauer Disk Diffusion Susceptibility Test method, as described by Loo et al. [9], was used with minor modifications to perform the antimicrobial activity of green synthesized AgNPs. The freshly cultured strains were spread on the MHA. About 10 µL of fermented and unfermented bush tea leaf extract, AgNO₃ solution (10 mM), AgNPs, and 50 mg/mL ampicillin (as positive control) were filled into the sterile blank antimicrobial susceptibility disks separately. The negative control was sterile distilled water. A black marker was used to mark where each disk was to be placed on the Petri dish to avoid confusion. The loaded disks were each placed on their respective mark on the MHA plate and incubated at 37 °C for 24 h. A clear zone was observed around the colonies, and the results were tabulated. All tests were carried out in triplicate, and the average result was taken.

2.6.3. Minimum Inhibitory Concentration (MIC)

The CLSI guideline method [37] was used to determine the MIC of fermented and unfermented AgNPs. A 96-well flat-bottom microtiter plate was used to determine the MIC using standard broth microdilution methods. About 100 µL MHB was added to all microtiter plate wells from column 1 to column 12. Columns 1 to 3 contained bacterial inoculums (10⁵ CFU/mL) and the fermented AgNPs solution (250 µg/mL) diluted two-fold. Columns 4 to 6 contained the bacterial inoculums (10⁵ CFU/mL), and the unfermented AgNPs solution diluted two-fold. Columns 7 and 8 contained unfermented and fermented AgNP solutions, respectively. Column 10 contained AgNPs solution and bacterial inoculums. Column 12 was the negative control containing only broth, and column 11 was a positive control containing broth and bacterial inoculums. About 30 µL of the resazurin solution was added to each microtiter plate well. The microtiter plates were incubated at 37 °C for 24 h, and color changes were observed. White or colorless indicates microbial growth, and blue or purple indicates no microbial growth.

2.6.4. Minimum Bactericidal Concentration (MBC)

About 50 µL of suspension from each well containing no microbial growth was transferred to the MHA. The MHA plates were then incubated at 37 °C for 24 h. The MBC value was the lowest concentration without noticeable growth on the MHA plate.

2.7. Statistical Analysis

The experiment was duplicated on different days. All data are expressed as the mean value of three independent triplicates ± the standard deviation (SD). The data were analyzed using SPSS software, version 26. Fisher's least significant difference test was used to determine significant mean differences when a *p*-value < 0.05 was found.

3. Results and Discussion

3.1. Visual Observation and UV-Visible Spectroscopy of the Green Synthesized Silver Nanoparticles

The color of the fermented AgNPs solution changed from black to dark brown, and the unfermented AgNPs solution changed from dark brown to light brown after 10 min (Figure 1A,B), indicating the successful formation of AgNPs [38]. Furthermore, there were no further color changes after incubation of the samples for 24 h because the Ag^+ silver metal ions were reduced to Ag^0 silver nanoparticles. This showed that the bioactive compounds available in the bush tea leaf extract, such as polyphenols, flavonoids, and tannins [9], might be accountable for reducing the $\text{Ag}(\text{I})$ ions and the capping of the subsequent AgNPs. Due to their interactions with metallic ions through their carbonyl functional groups, flavonoids release reactive hydrogen, which, in turn, causes the flavonoid's enol to change to keto form and produce Ag^0 [39]. Moreover, the color change might be associated with surface plasmon vibration, an optical characteristic unique to metal nanoparticles [40].

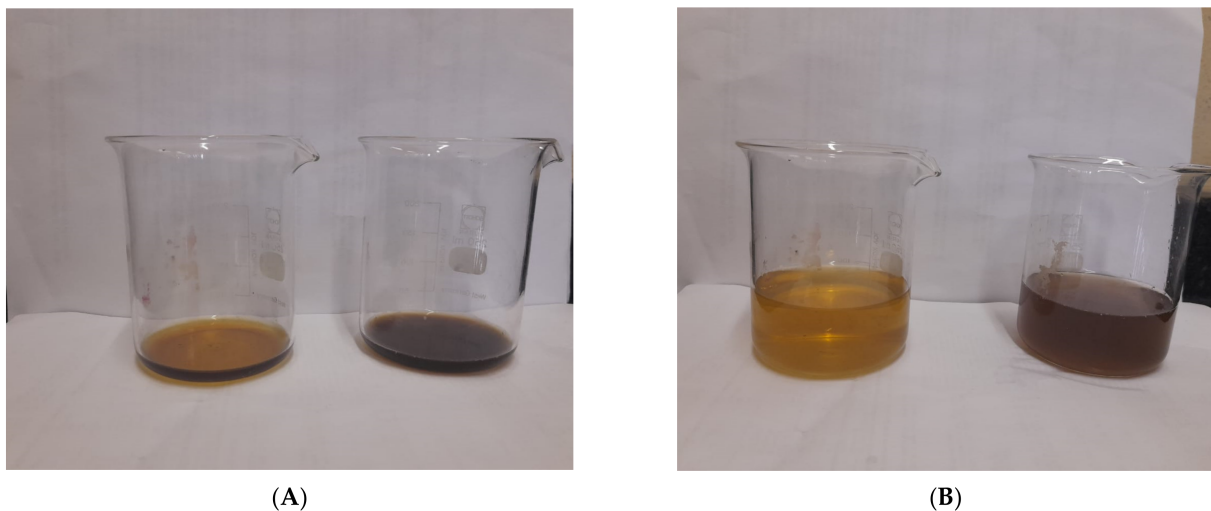


Figure 1. (A) (Left) unfermented bush tea leaf extract before adding 1 mM AgNO_3 and (Right) fermented bush tea leaf extract before adding 1 mM AgNO_3 . (B) (Left) unfermented bush tea leaf extract after adding 1 mM of AgNO_3 and (Right) fermented bush tea leaf extract after adding 1 mM of AgNO_3 .

Loo et al. [2] reported the visual observation of the color change of the fermented AgNO_3 /tea extract solution from colorless to light brown and later to dark brown. Furthermore, Hoda et al. [41] observed the color change of the AgNO_3 /*Chamaemelum noble* extract solution from colorless to brownish.

UV-vis spectroscopy is a proven method for the characterization of AgNPs. Visual inspection and UV-vis spectrophotometric measurements of the surface plasmon resonance (SPR) band demonstrate the production of AgNPs [42]. The samples were observed under a UV-vis spectrophotometer for their maximum absorbance and wavelength to confirm AgNP formation. The SPR absorption band is formed due to the simultaneous vibration of free electrons in metal nanoparticles in resonance with light waves [43]. Fermented AgNPs had a broad spectrum, indicating that they contain large AgNPs (Figure 2A). The narrow spectrum indicates that they contain tiny nanoparticles. The synthesized fermented AgNPs were brown in an aqueous solution due to electron excitation and changes in the amount of electronic energy, confirming the reduction of Ag^+ to Ag^0 [44]. The emergence of absorption peaks at 450 nm in fermented AgNPs and 457 nm in unfermented AgNPs (Figure 2B) detected by UV-vis spectroscopy indicates AgNPs formation.

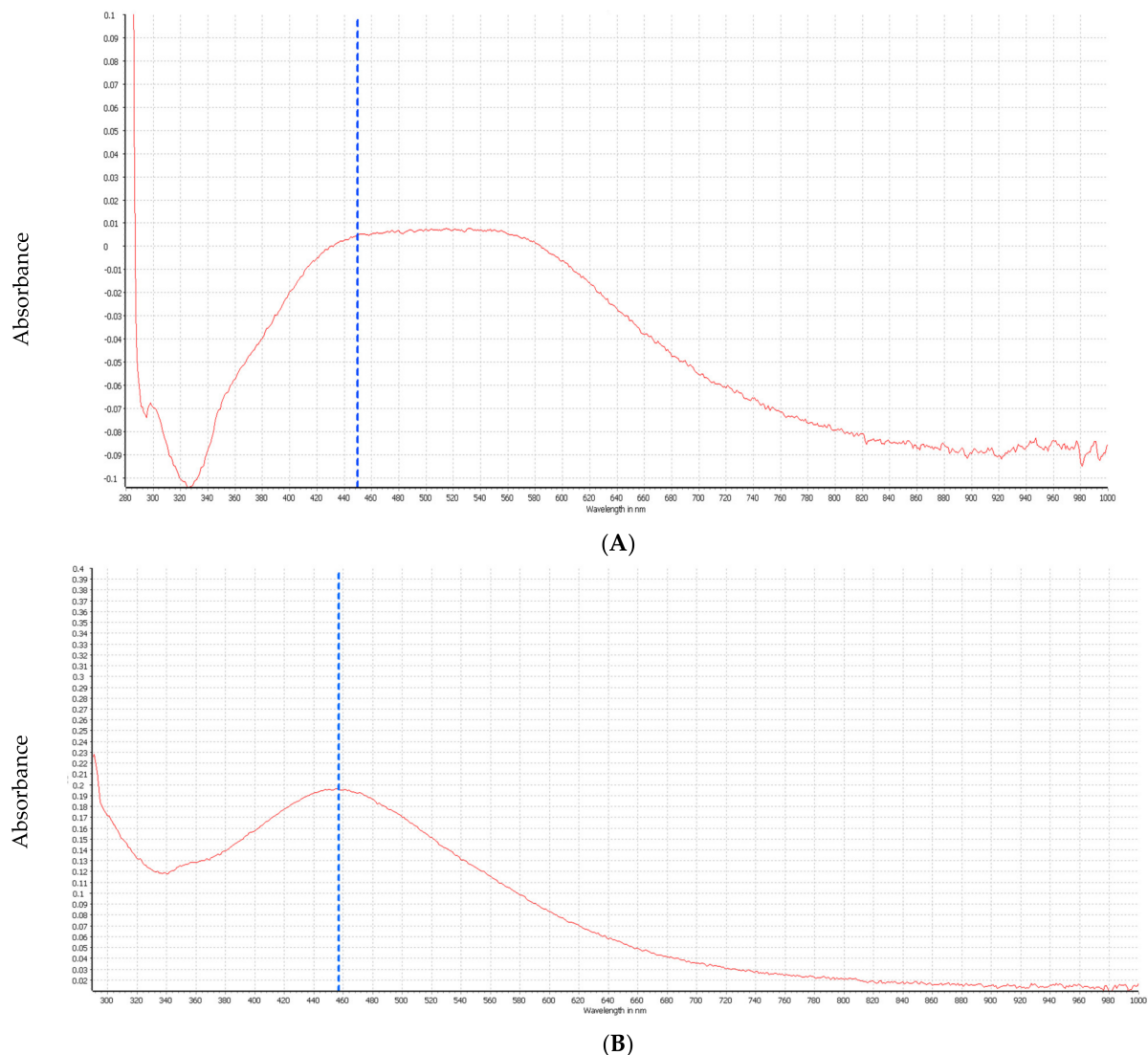


Figure 2. UV-vis of (A) Fermented green synthesized silver nanoparticles and (B) unfermented green synthesized silver nanoparticles produced by using bush tea leaf extract. The blue line shows maximum absorption peak while red line shows wavelength (nm).

The creation of a single peak in both green synthesized AgNPs shows the synthesis of spherical silver nanoparticles [43]. Different researchers have conducted similar studies using UV-vis, including the aqueous extract of *Satureja* by Somaye et al. [45]. The peak of synthesized AgNPs was observed at 475 nm in the UV-vis spectrum. Tea leaves extracted from *Camellia sinensis* peaked at a wavelength of 436 nm [2]. The extract of the *Gymnema sylvestre* leaf revealed the absorbance of the synthesized AgNPs at 442 nm [46].

3.2. FTIR Analysis of Green Synthesized Silver Nanoparticles

FT-IR analysis determined the functional groups responsible for the decrease in Ag^+ ions and the stabilization of the synthesized AgNPs in the leaf extract of bush tea [47]. The functional groups involved in the interaction between metal particles and biomolecules that contribute to the bioreduction, capping, and stabilizing of AgNPs can be easily identified using FTIR. Figure 3A,B shows the FTIR spectrum for AgNPs synthesized by fermented and unfermented bush tea leaf extract, respectively. As observed in Figure 3A, a broad peak at 3329 cm^{-1} might correspond to the hydroxyl groups ($-\text{OH}$) in polyphenols in bush tea, such as flavonoids and phenolic acids or $-\text{NH}$ stretch of amino groups [9]. The peak at 1636 cm^{-1} is the result of aromatic $\text{C}=\text{C}$ bending. Similarly, AgNPs synthesized

from unfermented bush tea (Figure 3B) showed a strong absorption peak at 3315 cm^{-1} , presumably resulting from the presence of OH groups or the stretching of the NH band of amino groups [48]. The relevant peaks observed in Figure 3B are strong absorption. The intense band at 2114 cm^{-1} results from $\text{C}\equiv\text{C}$ terminal alkyne. The intense band at 1636 cm^{-1} was a result of aromatic $\text{C}=\text{C}$ bending. The FTIR study showed that bush tea leaf extracts contain hydroxyl (OH) or amine (NH) groups; the amine group acts as a stabilizer, while the hydroxyl group contributes to the reduction of Ag^+ ions in Ag^0 nanoparticles because it acts as a reducing agent as it substitutes flavonoids [49].

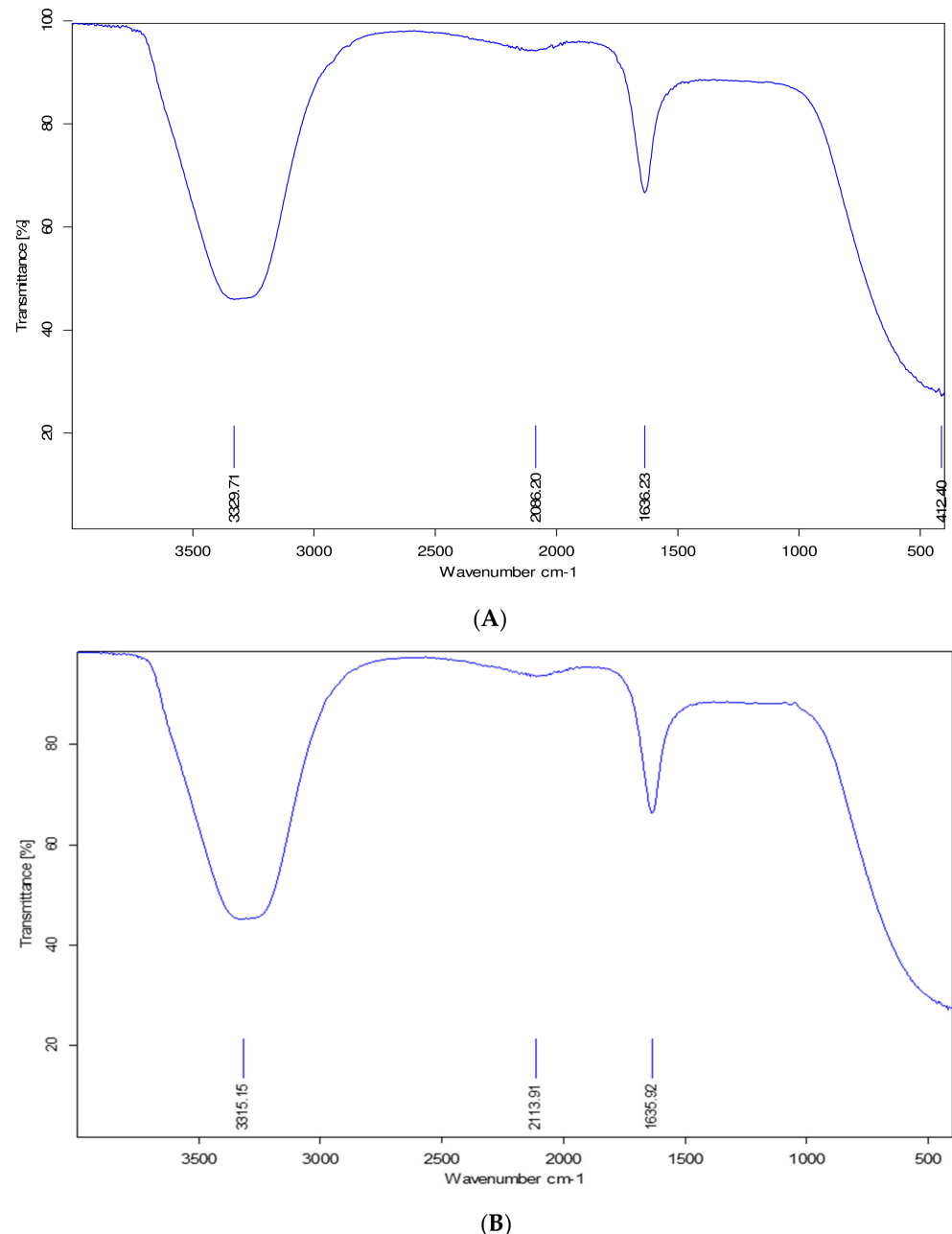


Figure 3. The FTIRs of (A) Fermented greenly synthesized silver nanoparticles and (B) unfermented greenly synthesized silver nanoparticles produced by using bush tea leaf extract.

FTIR spectroscopic investigations further revealed that the leaf extract of bush tea prevents agglomeration of AgNPs because it functions as a stabilizer [33]. The N-H bond of the amine and the $\text{C}=\text{C}$ stretch of the alkenes, respectively, suggest that proteins and phenolic compounds bind and stabilize molecules by generating AgNPs [50]. Tahir et al. [51]

observed the functional group alcohol, phenolic group, carbonyl, and aromatic stretching while studying the FTIR of AgNPs from *Artemisia vulgaris* tea extract. Vasudeo and Priya [52] also studied the FTIR spectra of biosynthesized AgNPs using cinnamon and observed a peak that indicated that the O-H stretching group of phenols, alcohols, and carbonyl groups were present.

3.3. Differential Scanning Calorimetry of Green Synthesized Silver Nanoparticles

Differential scanning calorimetry (DSC) is an analytical method that uses the function of temperature (reference) to measure the amount of heat required to increase the temperature of the sample. According to Table 1, fermented AgNPs had an onset temperature of 62.45 °C while unfermented AgNPs had 48.01 °C. Furthermore, fermented AgNPs showed an endothermic peak at 48.48 °C, and unfermented AgNPs peaked at 39.18 °C. The weight loss of AgNPs occurred at a temperature below 100 °C; thus, the denaturing temperature for fermented and unfermented AgNPs suggests that low thermal stable compounds contributed to the reduction of Ag⁺ to Ag⁰ due to phyto compounds found in the bush tea leaf extract.

Table 1. Thermal properties of fermented and unfermented bush tea nanoparticles.

Sample	To (°C)	Tp (°C)	Tc (°C)	Delta H
Fermented AgNPs	62.45 ± 14.16 ^b	48.48 ± 12.88 ^a	79.27 ± 14.67 ^a	4.39 ± 5.15 ^a
Unfermented AgNPs	48.01 ± 4.17 ^a	39.18 ± 8.30 ^b	59.26 ± 17.01 ^b	11.98 ± 8.26 ^b

Values are expressed as mean ± standard deviation. Values followed by different small letters in the same column indicate a statistically significant difference at $p < 0.05$. To = Onset temperature. Tp = peak temperature, Tc = conclusion temperature, Delta H = enthalpy of gelatinization.

The melting temperature of fermented AgNPs was 48.48 °C, while that of unfermented AgNPs was 39.18 °C. Fermented AgNPs contain larger sample masses than unfermented AgNPs because large sample masses and higher heating rates shift the peak to higher temperatures. AgNPs from fermented and unfermented bush tea leaf extract required 4.39 °C and 11.98 °C to melt the solid particles, respectively. Rajeswari et al. [53] conducted a similar experiment using the *Coccinia grandis* leaf extract and reported that the synthesized AgNPs showed an endothermic peak at 65 °C. Rohan and Anup [54] used sundried *Kalanchoe pinnata* leaf extract and reported that the synthesized AgNPs showed an endothermic peak at 123.99 °C.

3.4. Antioxidant Properties of Green Synthesized Silver Nanoparticles

The results show that the bush tea leaf extract contained 165.46 mg/100 g GAE (Figure 4A) of the total phenolic content (TPC) and 14.89 mg/100 g CE of total flavonoid content (TFC) (Figure 4B). The TPC of the bush tea leaf extract was low compared to the fermented and unfermented AgNPs. On the other hand, the TFC of the leaf extract was higher than that of the fermented AgNPs. Nevertheless, the presence of these compounds on the synthesized AgNPs demonstrated the role of the polyphenolic compounds as the reducing agents in the generation of AgNPs [55]. Mohamed et al. [56] studied the TPC of synthesized AgNPs using *Chenopodium murale* leaf extract and observed that the TPC was higher in plant-AgNPs than in aqueous extract. On the other hand, Fafal [57] studied the TPC of synthesized AgNPs using *Asphodelus aestivus* Brot. aerial part extract showed that the TPC was higher in the aqueous extract than in the plant-AgNPs. AgNPs synthesized by leaf extract of *Ocimum tenuiflorum* had high TFC, but TPC was high in leaf extract and low in AgNPs [58].

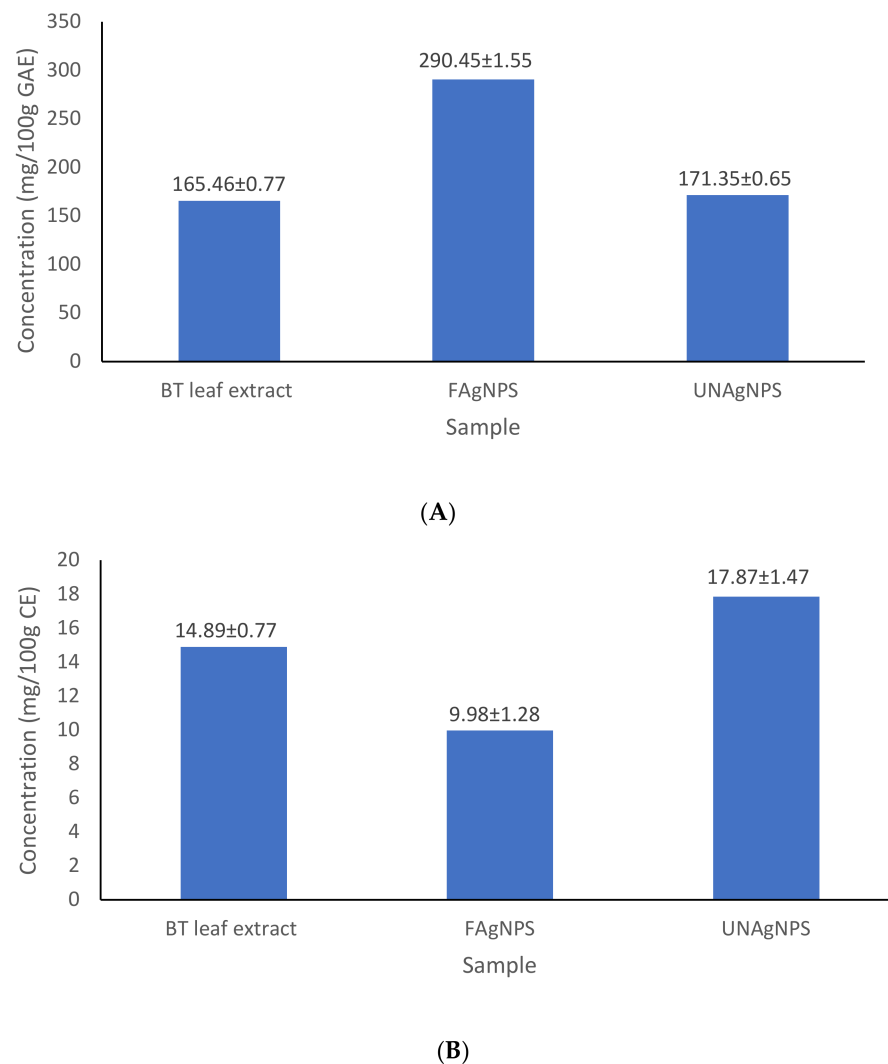


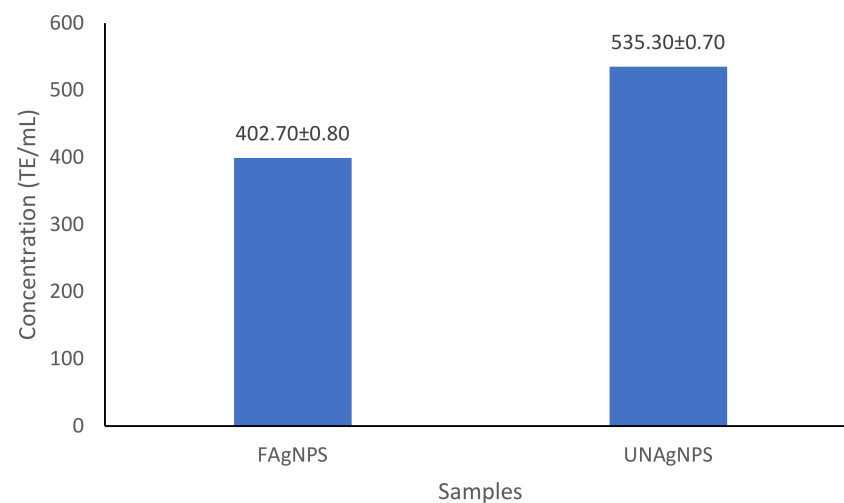
Figure 4. (A) Total phenolic content of bush tea leaf extract, fermented and unfermented bush tea silver nanoparticles; (B) Total flavonoid content of bush tea leaf extract, fermented and unfermented bush tea silver nanoparticles. FAgNPS = Fermented AgNPS, UNAgNPS = Unfermented AgNPS, and BT = Bush tea.

The fermented AgNPs reaction solution had the highest TPC (290 mg/100 g GAE). Unfermented AgNPs reaction solution had a value of 171.35 mg/100 g GAE, as shown in Figure 4A. The TPC of fermented AgNPs was higher, indicating that the TPC increased during fermentation. Depolymerization of high molecular weight phenolic compounds and conversion of single phenolic compounds is aided by the availability of bacteria in fermentation [59]. Vorobyova et al. [60] demonstrated that phenolic compounds work well as a reducing agent in the production of nanoparticles. According to Nazarni et al. [59], the total phenols of plant extract or parts increase after fermentation.

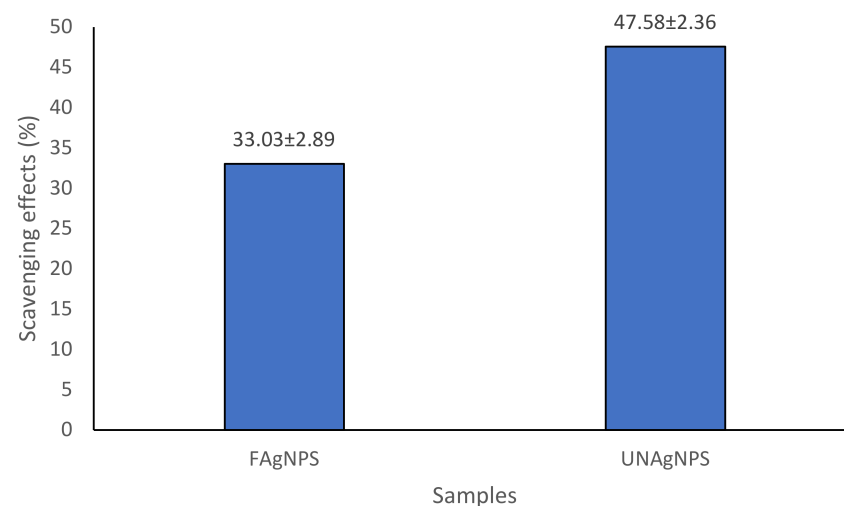
A high value of TFC (17.87 mg/100 g CE) was observed in the reaction solution of unfermented AgNPs, while a minimum value (9.98 mg/100 g CE) value was observed in fermented AgNPs (Figure 4B). The results show that during fermentation, flavonoids decreased. The low TFC in the fermented AgNPs reaction solution might be attributed to the degradation of phenolic compounds during fermentation, causing a significant loss of flavonoids [61]. During fermentation, the bacteria release extracellular enzymes into the extract that break phenolic compounds such as flavonoids and tannins, leading to their decrease. Mohamed et al. [56] studied the TFC of synthesized AgNPs using *Chenopodium*

murale leaf extract and observed that the TFC was higher in plant-AgNPs than in the aqueous extract.

The FRAP method measures the total antioxidant capacity because, under acidic conditions, antioxidants reduce Fe^{3+} to Fe^{2+} . When the glycosidic bond breaks, the reducing sugar increases, improving the degraded polysaccharides' reducibility [61]. The reducing ability of the fermented and unfermented AgNPs reaction solution was determined using the FRAP assay. The reaction solution of unfermented AgNPs had the highest antioxidant activity of 535.29 TE/mL, while fermented AgNPs had the minimum antioxidant activity (402.70 TE/mL), as shown in Figure 5A. Thermosensitive antioxidant compounds are damaged by temperature, resulting in low FRAP values of fermented AgNPs [62].



(A)



(B)

Figure 5. (A) FRAP assay of fermented and unfermented greenly synthesized silver nanoparticles produced by using bush tea leaf extract; (B) DPPH of fermented and unfermented greenly synthesized silver nanoparticles produced by using bush tea leaf extract. FAGNPs = Fermented AgNPs, and UNAgNPs = Unfermented AgNPs.

Similarly, Rabeta and Lai [63] studied *Ocimum tenuiflorum* tea and reported that unfermented tea had the highest FRAP value, translating to the highest antioxidant activity.

De Marco Castro et al. [62] reported that *Spirulina (Arthrospira platensis)* decreased after fermentation, possibly due to damage to air and heat-sensitive antioxidants.

DPPH can be used as a chemical to monitor radicals in antioxidant analysis or to chemically monitor the position and strength of the paramagnetic electron resonance signal. In the DPPH assay (Figure 5B), the unfermented AgNPs reaction solution had the highest antioxidant activity of 47.58%, while the fermented AgNPs reaction solution had the minimum antioxidant activity (33.03%). The highest antioxidant activity of unfermented AgNPs is probably linked to the adsorption of phytochemicals over ball-shaped AgNPs [43]. The results indicate that unfermented AgNPs are the most effective scavenger against DPPH compared to fermented AgNPs.

3.5. Antimicrobial Activity by the Agar Diffusion Method

Fermented, unfermented AgNPs and AgNO₃ were tested against two Gram-positive (*S. epidermidis* ATCC 12228 and *B. cereus* ATCC 10876), one Gram-negative (*E. coli* ATCC 25922) bacteria, and one fungus (*C. albicans* ATCC 10231). When only bush tea leaf extract was used, no inhibition zone was observed, indicating that bush tea leaf extract did not have anti-bacterial activity against the four microorganisms tested (Figure 6). This may be due to the low amount of leaf extract. In the AgNO₃ solution, a distinct inhibition zone of varying diameter appeared against all tested microorganisms. Most bacterial isolates were sensitive to the fermented AgNPs reaction solution, as shown in Table 2. *S. epidermidis* was more sensitive to the unfermented AgNPs reaction solution than other bacterial strains. The diameter zone of inhibition of the unfermented AgNPs reaction solution ranged from 10.45 mm to 15.88 mm. The zone of inhibition of *S. epidermidis* was 15.88 mm, while the zones of inhibition for *B. cereus*, *E. coli*, and *C. albicans* were 10.73 mm, 10.45 mm, and 10.79 mm, respectively. When a clear zone appears around the well, it shows that bacteria growth was inhibited.

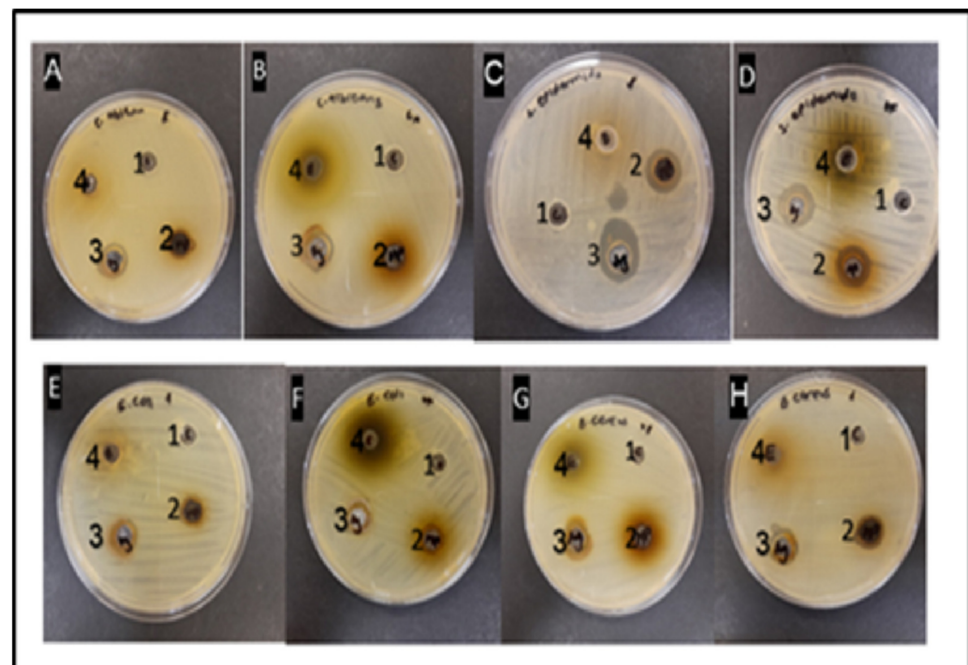


Figure 6. Images of the well diffusion results (A,B) *C. albicans*, (C,D) *S. epidermidis*, (E,F) *E. coli*, (G,H) *B. cereus*. In terms of numbers, 1 = distilled water as control, 2 = silver nanoparticles, 3 = silver nitrate only, and 4 = extract only.

Table 2. Antimicrobial activity of fermented and unfermented bush tea nanoparticles by Agar well diffusion method.

Microorganisms	Zone of Inhibition (mm *)		
	Unfermented AgNPs	Fermented AgNPs	AgNO ₃
<i>B. cereus</i>	10.73 ± 0.18 ^a	13.28 ± 0.25 ^a	11.87 ± 1.17 ^a
<i>S. epidermidis</i>	15.88 ± 0.34 ^b	14.33 ± 2.69 ^b	13.55 ± 2.14 ^b
<i>E. coli</i>	10.45 ± 0.39 ^a	12.03 ± 0.69 ^a	11.27 ± 0.41 ^a
<i>C. albicans</i>	10.79 ± 0.18 ^a	12.09 ± 0.38 ^a	12.45 ± 0.55 ^a

* Diameter of the inhibition zones in mm (include 7 mm borer). Values are expressed as mean ± standard deviation. Values followed by different small letters in the same column indicate a statistically significant difference at $p < 0.05$.

Unfermented AgNPs were less effective than AgNO₃ in *B. cereus*, *E. coli*, and *C. albicans* and more effective in *S. epidermidis*. Meanwhile, the fermented AgNPs solution showed excellent anti-bacterial and anti-fungal properties compared to that of the unfermented AgNPs solution. The most significant effect of fermented AgNPs was on *S. epidermidis*, with an average inhibition zone of 14.33 mm. The organisms: *B. cereus*, *E. coli*, and *C. albicans* had an inhibition zone diameter of 13.28 mm, 12.03 mm, and 12.09 mm, respectively. The fermented AgNPs worked better than both the unfermented AgNPs and AgNO₃.

3.6. Antimicrobial Activity by the Kirby–Bauer Disc Diffusion Method

The positive control in the Kirby–Bauer disc diffusion test technique was ampicillin (10 mg/mL), while the negative control was sterile distilled water. The diffusion of agar and the diffusion of discs (Table 3) showed that the fermented and unfermented AgNP solutions had excellent antimicrobial properties against the tested microorganisms. Similarly, AgNPs made from wild *Cucumis anguria* displayed anti-bacterial efficacy against pathogenic bacterial strains [64]. The unfermented AgNPs inhibition zone ranged from 7.71 to 9.41 mm. *S. epidermidis* was more sensitive with a zone of inhibition of 9.41 mm, while *C. albicans* were the least sensitive, with a zone of 7.71 mm. *B. cereus* and *E. coli* had inhibition zones of 8.60 mm and 8.74 mm.

Table 3. Antimicrobial activity of fermented and unfermented bush tea nanoparticles by disk diffusion method.

Microorganisms	Zone of Inhibition (mm *)			
	Unfermented AgNPs	Fermented AgNPs	AgNO ₃	Ampicillin
<i>B. cereus</i>	8.60 ± 0.34 ^a	8.97 ± 2.02 ^a	8.60 ± 1.24 ^a	0
<i>S. epidermidis</i>	9.41 ± 0.37 ^a	10.16 ± 2.44 ^a	7.82 ± 0.93 ^a	7.00 ± 1.09 ^a
<i>E. coli</i>	8.74 ± 0.95 ^a	9.17 ± 0.56 ^a	8.17 ± 1.11 ^a	9.05 ± 1.96 ^b
<i>C. albicans</i>	7.71 ± 1.76 ^a	9.06 ± 1.74 ^a	8.57 ± 1.49 ^a	6.93 ± 1.94 ^a

* Diameter of the inhibition zones in mm (include 6 mm disc). Values are expressed as mean ± standard deviation. Values followed by different small letters in the same column indicate a statistically significant difference at $p < 0.05$.

For the fermented AgNPs solution, *S. epidermidis* was still more sensitive with a diameter of the inhibition zone of 10.16 mm, while *B. cereus* was the least sensitive, with a zone of 8.97 mm. *E. coli* and *C. albicans* had inhibition zones of 9.17 mm and 9.06 mm, respectively. Ampicillin is a semisynthetic penicillin antibiotic that is used to treat bacterial infections such as urinary, gastrointestinal, and respiratory tract infections [65]. *E. coli* was highly sensitive to ampicillin, with 9.05 mm as the diameter zone of inhibition, while *B. cereus* was resistant. The zone of inhibition for *S. epidermidis* strain and *C. albicans* were 7.00 mm and 6.93 mm, respectively.

The agar diffusion method outperformed the disc diffusion method in antimicrobial activity. The size of AgNPs plays an important role in the antimicrobial effectiveness of the nanoparticles. Smaller nanoparticles have greater ability and antimicrobial activity. This is because smaller nanoparticles have a larger surface area, allowing greater interaction and

ascending intracellular penetration [66]. Studies on the antimicrobial efficiency of AgNPs against various pathogens vary depending on the reduction method, concentration, size, and shape of AgNPs [67]. It is noted from the results of the agar well method that AgNPs are less effective in Gram-negative bacteria (*E. coli*) and more effective in Gram-positive bacteria (*S. epidermidis* and *B. cereus*) and fungi (*C. albicans*). This might be attributed to the differences in their cell wall composition. Although Gram-negative bacteria are composed of a single layer of peptidoglycan in their cell membrane, their outer membrane acts as a protective barrier by inhibiting and/or delaying the penetration of AgNPs.

On the other hand, a Gram-positive cell membrane comprises a complex peptidoglycan, making it more rigid for penetration; however, its thick selective permeable membrane absorbs antibiotics and most cleaning products, making it easier to kill [68]. The low/slightly negative charges on the bacterial cell wall attract silver cations from nanoparticles, and the Ag⁺ ions cause a change in the composition of the cell wall, which affects its permeability [69]. Due to this attraction and activity, the internal environment of the cell and the membrane polarization change, resulting in cell death [11,22]. When microbes are exposed to Ag⁺ ions, their DNA tends to replicate, the enzymes that help produce ATP are inhibited, and the expression of ribosome subunit proteins and other proteins that are found in the cell become inactivated [65].

3.7. Minimum Inhibitory Concentration and Minimum Bactericidal Concentration of Green Synthesized Silver Nanoparticles

The minimum inhibitory concentration (MIC) value was established as the lowest antimicrobial agent concentration necessary to suppress the growth of bacteria by serial dilution. The unfermented AgNPs had MIC values ranging from 62.25 to 72.91 µg/mL, as shown in Table 4. *S. epidermidis* and *E. coli* showed 62.25 µg/mL, *B. cereus* and *C. albicans* showed 72.91 µg/mL. The MIC results of fermented AgNPs ranged from 4.85 to 83.33 µg/mL; *S. epidermidis* showed the highest activity at 4.85 µg/mL, while *C. albicans* displayed the lowest activity with a MIC of 83.33 µg/mL. Minimum bactericidal concentration (MBC) is the lowest concentration of antimicrobial agent needed to kill a microbe. The concentration of AgNPs showing no microbial growth on the agar is considered the MBC. The MBC values of unfermented AgNPs varied from 62.5 to 125 µg/mL, as shown in Table 4. *S. epidermidis* and *E. coli* were 62.5 µg/mL, and *B. cereus* was 125 µg/mL.

Table 4. MIC value (µg/mL), and MBC value (µg/mL) of fermented and unfermented bush tea nanoparticles.

Microorganisms	Unfermented AgNPs		Fermented AgNPs	
	MIC (µg/mL)	MBC (µg/mL)	MIC (µg/mL)	MBC (µg/mL)
<i>B. cereus</i>	72.91 ± 47.69 ^b	125 ± 0.00 ^c	52.08 ± 18.4 ^b	62.5 ± 0.00 ^b
<i>S. epidermidis</i>	62.5 ± 0.00 ^a	62.5 ± 0.00 ^a	4.85 ± 1.15 ^a	7.9 ± 0.00 ^a
<i>E. coli</i>	62.5 ± 0.00 ^a	62.5 ± 0.00 ^a	41.66 ± 18.04 ^b	62.5 ± 0.00 ^b
<i>C. albicans</i>	72.91 ± 47.7 ^b	72.91 ± 0.00 ^b	83.33 ± 36.15 ^c	125 ± 0.00 ^c

Values are expressed as mean ± standard deviation. Values followed by different small letters in the same column indicate a statistically significant difference at *p* < 0.05.

The MBC results of fermented AgNPs ranged from 7.9 to 125 µg/mL; once again, *S. epidermidis* showed the highest activity at 7.9 µg/mL, while *C. albicans* displayed the lowest activity with an MBC value of 83.33 µg/mL.

The MIC and MBC results show that *S. epidermidis* is more susceptible to fermented AgNPs. Overall, the solution with fermented bush tea synthesized AgNPs was more effective than the unfermented AgNPs. Many studies hypothesized that the anti-bacterial activity of AgNPs was related to their capacity to infiltrate and disrupt cells [6], the breakdown of the cell wall and cell membrane, oxidative stress, the concentration of AgNPs, and even the biochemicals found in the extract [67,70].

In comparison to fermented AgNPs, the unfermented AgNPs solution was less effective. The larger surface area of fermented AgNPs, which increases their surface availability for surface interactions and enhances their bactericidal effects, may have contributed to their increased anti-bacterial activity [7]. Moreover, this could be due to the availability of a powerful reductant in the fermented extract, which facilitates a rapid reaction rate and the development of smaller nanoparticles in size [70]. Plants contain terpenoids, alkaloids, flavonoids, sugars, proteins, polyphenols, and steroids that act as reducing and stabilizing agents during the generation of nanoparticles [71].

4. Conclusions

Silver nanoparticles were effectively produced using the leaf extract of bush tea. This inexpensive and eco-friendly leaf extract of bush tea served as a potential stabilizing and reducing agent. The production of AgNPs was confirmed by a color change from brown to light brown and black to brown due to the SPR peak in the UV-vis spectra observed at 450 and 457 nm. FTIR spectroscopy confirmed the presence of functional biomolecules. During fermentation, the total phenolic content of AgNPs increases, while the total flavonoid content decreases. Fermenting bush tea for an extended period decreases the antioxidant activity of AgNPs. Therefore, unfermented AgNPs are the most effective scavenger against DPPH and FRAP antioxidant activities. *S. epidermidis* was more vulnerable to fermented AgNPs than the other opportunistic microbes, while *E. coli* was less vulnerable to fermented and unfermented AgNPs. Fermented AgNPs have more antimicrobial activity than unfermented AgNPs. Thus, the green synthesized AgNPs from fermented bush tea leaf extract is a viable alternative to investigate ways to combat infectious diseases.

Author Contributions: Conceptualization, M.E.M., M.L.R. and F.N.M.; Methodology, M.E.M., T.M. and K.F.; Software, F.N.M., M.L.R. and M.E.M.; Formal analysis, M.E.M., M.L.R., F.N.M., T.M., K.F. and B.N.; Investigation, M.E.M., T.M., K.F., B.N. and M.L.R.; Resources, M.E.M., M.L.R. and F.N.M.; Data curation, M.E.M., B.N., T.M., K.F. and F.N.M.; Writing—T.M., K.F. and M.E.M.; Writing—review and editing, M.E.M., M.L.R., B.N. and F.N.M. All authors have read and agreed to the published version of the manuscript.

Funding: This research received no external funding.

Institutional Review Board Statement: Not applicable.

Informed Consent Statement: Not applicable.

Data Availability Statement: The data presented in this study are available on request from the corresponding author.

Conflicts of Interest: The authors declare no conflict of interest.

References

1. Arumugam, S.; Jeyaraman, J.; Pappu, S. Green synthesis of silver nanoparticles using *Lippia nodiflora* aerial extract and evaluation of their antioxidant, anti-bacterial and cytotoxic effects. *Res.-Effic. Technol.* **2017**, *3*, 506–515.
2. Loo, Y.Y.; Buong, W.C.; Mitsuaki, N.; Son, R. Synthesis of silver nanoparticles by using tea leaf extract from *Camellia sinensis*. *Int. J. Nanomed* **2012**, *7*, 4263–4267.
3. Saba, F.; Abudul, M.O.; Nazoora, K.; Mohd, S.U. Fabrication of microbicidal silver nanoparticles: Green synthesis and implications in the containment of bacterial biofilm on orthodontal appliances. *Front. Nanotechnol* **2022**, *4*, 780783.
4. Mohammed, R.S.; Mujeeb, K.; Mufsir, K.; Abdulrahman, A.; Hamad, Z.A.; Mohammed, R.H.S.; Jilani, P.; Shaik, A.A.; Adeem, M.; Merajuddin, K.; et al. Plant-extract-assisted green synthesis of silver nanoparticles using *Origanum vulgare* L. extract and their microbicidal activities. *Sustainability* **2018**, *10*, 913.
5. Fouda, A.; Awad, M.A.; AL-Faifi, Z.E.; Gad, M.E.; Al-Khalaf, A.A.; Yahya, R.; Hamza, M.F. *Aspergillus flavus*-mediated green synthesis of silver nanoparticles and evaluation of their anti-bacterial, anticandida, acaricides, and photocatalytic activities. *Catalysts* **2022**, *12*, 462. [[CrossRef](#)]
6. Huston, M.; DeBella, M.; DiBella, M.; Gupta, A. Green synthesis of nanomaterials. *Nanomaterials* **2021**, *11*, 2130. [[CrossRef](#)]
7. Badawy, A.A.; Abdelfattah, N.A.H.; Salem, S.S.; Awad, M.F.; Fouda, A. Efficacy assessment of biosynthesized copper oxide nanoparticles (CuO-NP) in stored grain insects and their impacts on morphological and physiological traits of wheat (*Triticum aestivum* L.). *Plant. Biol.* **2021**, *10*, 233. [[CrossRef](#)]

8. Arintonang, H.F.; Koleangan, H.; Wuntu, A.D. Synthesis of silver nanoparticles using aqueous extract of medicinal plants' (*Impatiens balsamina* and *Lantana camara*) fresh leaves and analysis of antimicrobial activity. *Int. J. Microbiol.* **2019**, *2019*, 8642303. [[CrossRef](#)]
9. Loo, Y.Y.; Rukayadi, Y.; Nor-Khaizura, M.A.R.; Kuan, C.H.; Chieng, B.W.; Nishibuchi, M.; Radu, S. In vitro antimicrobial activity of green synthesized silver nanoparticles against selected gram-negative foodborne pathogens. *Front. Microbiol.* **2018**, *9*, 1555. [[CrossRef](#)]
10. Martínez Espinosa, J.C.; Carrera Cerritos, R.; Ramírez Morales, M.A.; Sánchez Guerrero, K.P.; Silva Contreras, R.A.; Macías, J.H. Characterization of silver nanoparticles obtained by a green route and their evaluation in the bacterium of *Pseudomonas aeruginosa*. *Crystals* **2020**, *10*, 395. [[CrossRef](#)]
11. Yuan, Y.-G.; Peng, Q.-L.; Gurunathan, S. Effects of silver nanoparticles on multiple drug-resistant strains of *Staphylococcus aureus* and *Pseudomonas aeruginosa* from mastitis-infected goats: An alternative approach for antimicrobial therapy. *Int. J. Mol. Sci.* **2017**, *18*, 569. [[CrossRef](#)]
12. Malongane, F.; McGaw, L.J.; Nyoni, H.; Mudau, F.N. Metabolic profiling of four South African herbal teas using high resolution liquid chromatography-mass spectrometry and nuclear magnetic resonance. *Food Chem.* **2018**, *257*, 90–100. [[CrossRef](#)]
13. Kumar, V.; Bano, D.; Mohan, S.; Singh, D.K.; Hassan, S.H. Sunlight induced green synthesis of silver nanoparticles using aqueous leaf extract of *Polyalthia longifolia* and its antioxidant activity. *Mater. Lett.* **2016**, *181*, 371–377. [[CrossRef](#)]
14. Manasa, D.J.; Chandrashekar, K.R.; Madhu Kumar, D.J.; Niranjana, M.; Meghana Navada, K. *Mussaenda frondosa* L. mediated facile green synthesis of copper oxide nanoparticles—Characterization, photocatalytic and their biological investigations. *Arab. J. Chem.* **2021**, *14*, 103184. [[CrossRef](#)]
15. Nagaraja, S.; Govindarajan, K.; Kalyanaraman, R.; Arvindganth, R.; Bose, R.; Bandar, E.A.; Venugopala, N.; Mahesh, A.; Anroop, B.N.; Rajith, K.K.; et al. Synthesis, characterization, and biological activity of silver nanoparticles synthesized from *Aristolochia bracteolata* lam. *Pharmacogn. Mag.* **2020**, *16*, 568–573.
16. Kiranmai, M. Biological and non-biological synthesis of metallic nanoparticles. *Indian J. Pharm. Sci.* **2017**, *79*, 501–512.
17. Saleh, G.M.; Najim, S.S. Anti-bacterial activity of silver nanoparticles synthesized from plant latex. *Iraqi J. Sci.* **2020**, *61*, 1579–1588. [[CrossRef](#)]
18. Muhammad, R.; Iqra, S.; Shahid, M.R.; Bilal, T.M. A review on green synthesis of silver nanoparticles and their applications. *Artif. Cells. Nanomed. Biotechnol.* **2016**, *45*, 1272–1291.
19. Karthik, N.; Ponnusamy, P.; Balasubramanian, M.G.; Mani, S.; Shivasji, K. Biosynthesis of silver nanoparticles from *Streptomyces* Spp., characterization and evaluating of its efficacy against *Phomopsis theae* and *Poria hypolateraria* in tea plants (*Camellia sinensis*). *Nano Biomed. Eng.* **2020**, *12*, 272–280.
20. Bello, B.A.; Khan, S.A.; Khan, J.A.; Syed, F.Q.; Mirza, M.B.; Shah, L.; Khan, S.B. Anticancer, anti-bacterial, and pollutant degradation potential of silver nanoparticles from *Hyphaene thebaica*. *Biochem. Biophys. Res. Commun.* **2017**, *490*, 889–894. [[CrossRef](#)]
21. Ontong, J.C.; Paosen, S.; Shankar, S.; Voravuthikunchai, S.P. Eco-friendly synthesis of silver nanoparticles using *Senna alata* bark extract and its antimicrobial mechanism through enhancement of bacterial membrane degradation. *J. Microbiol. Methods* **2019**, *165*, 105692. [[CrossRef](#)] [[PubMed](#)]
22. Raj, S.; Mali, S.C.; Trivedi, R. Green synthesis and characterization of silver nanoparticles using *Enicostemma axillare* (Lam.) leaf extract. *Biochem. Biophys. Res. Commun.* **2018**, *503*, 2814–2819. [[CrossRef](#)] [[PubMed](#)]
23. Gopinath, V.; MubarakAli, D.; Priyadarshini, S.; Priyadharshini, N.M.; Thajuddin, N.; Velusamy, P. Biosynthesis of silver nanoparticles from *Tribulus terrestris* and its antimicrobial activity: A novel biological approach. *Colloids Surf. B Biointerfaces* **2012**, *96*, 69–74. [[CrossRef](#)] [[PubMed](#)]
24. Royhan Uddin, A.K.M.; Bakar Siddique, M.A.; Rahman, F.; Atique Ullah, A.K.M.; Khan, K. *Cocos nucifera* leaf extract mediated green synthesis of silver nanoparticles for enhanced anti-bacterial activity. *J. Inorg. Organomet Polym. Mater.* **2020**, *30*, 3305–3316. [[CrossRef](#)]
25. Hlahla, L.N.; Mudau, F.N.; Mariga, I.K. Effect of fermentation temperature and time on the chemical composition of bush tea (*Athrixia phylicoides* DC.). *J. Med. Plant Res.* **2010**, *4*, 824–829.
26. Mathivha, L.P.; Mudau, N.F. Response of total phenolic content and antioxidant activities of bush tea and special tea using different selected extraction solvents. *J. Consum. Sci.* **2017**, *45*, 27–33.
27. Lerotholi, L.; Chaudhary, S.K.; Combrinck, S.; Viljoen, A. Bush tea (*Athrixia phylicoides*): A review of traditional uses, bioactivity, and phytochemical. *South Afr. J. Bot.* **2017**, *110*, 4–17. [[CrossRef](#)]
28. Maedza, K.V.; Mpumelelo, N.; Wonde, N.; Nokwanda, P.M.; Mudau, F.N. Response of phytochemicals in bush tea (*Athrixia phylicoides* DC.) as influenced by selected micronutrients. *HortScience* **2017**, *52*, 965–971.
29. Ramphinwa, M.L.; Mchau, G.R.A.; Madala, N.E.; Nengovhela, N.; John, B.O.; Ogola, J.B.O.; Mudau, F.N. Response of plant growth and development, and accumulation of hydroxyl-cinnamoyl acid derivatives to selected shade nets and seasonality of field-grown bush tea (*Athrixia phylicoides* DC.). *HortScience* **2022**, *57*, 87–96. [[CrossRef](#)]
30. Kaningini, G.A.; Azizi, S.; Nyoni, H.; Mudau, F.N.; Mohale, K.C.; Maaza, M. Green synthesis and characterization of zinc oxide nanoparticles using bush tea (*Athrixia phylicoides* DC) natural extract: Assessment of the synthesis process. *F1000Research* **2022**, *10*, 1077. [[CrossRef](#)]

31. Ayinde, W.B.; Gitari, M.W.; Muchindu, M.; Samie, A. Biosynthesis of ultrasonically modified Ag-MgO nanocomposite and its potential for antimicrobial activity. *J. Nanotechnol.* **2018**, *56*, 5–16. [[CrossRef](#)]
32. Wang, D.; Xue, B.; Wang, L.; Zhang, Y.; Liu, L.; Zhou, Y. Fungus-mediated green synthesis of nano-silver using *Aspergillus sydowii* and its anti-fungal/antiproliferative activities. *Sci. Rep.* **2021**, *11*, 10356. [[CrossRef](#)]
33. Yadav, S.; Patil, S.H.; Patel, P.; Nair, V.; Khan, S.; Kakkar, S.; Durve, A. Green synthesis of silver nanoparticles from plant sources and evaluation of their antimicrobial activity. *Adv. Anal. Tools Mat. Charact.* **2018**, *5*, 133–139.
34. Akintola, A.O.; Kehinde, B.D.; Ayoola, P.B.; Adewoyin, A.G.; Adedose, O.T.; Ajayi, J.F.; Ogunsona, S.B. Antioxidant properties of silver nanoparticles biosynthesized from methanolic leaf extract of *Blighia sapida*. *IOP Conf. Ser. Mater. Sci. Eng.* **2017**, *805*, 012004. [[CrossRef](#)]
35. Souza, B.W.S.; Vincente, A.A. Chemical characterization and antioxidant activity of sulfated polysaccharide from the seaweed *Gracilaria birdiae*. *Food Hydrocoll.* **2012**, *27*, 287–292. [[CrossRef](#)]
36. Lin, S.; Cheng, Y.; Liu, J.; Wiesner, M.R. Polymeric coatings on silver nanoparticles hinder autoaggregation but enhance attachment to uncoated surfaces. *Langmuir* **2012**, *28*, 4178–4186. [[CrossRef](#)]
37. CLSI. *Performance Standards for Antimicrobial Susceptibility Testing; Twenty-Second Informational Supplement; The Clinical and Laboratory Standards Institute*: Wayne, PA, USA, 2012.
38. Mukaratirwa-Muchanyereyi, N.; Muchenje, T.; Nyoni, S.; Shumba, M.; Mupa, M.; Luke Gwatidzo, L.; Rahman, A. Green synthesis of silver nanoparticles using *Euphorbia confinalis* stem extract, characterization and evaluation of antimicrobial activity. *J. Nanomater. Mol. Nanotechnol.* **2017**, *6*, 3.
39. Melkamu, W.; Bitew, L.G. Green synthesis of silver nanoparticles using *Hagenia abyssinica* (Bruce) J.F. Gmel plant leaf extract and their anti-bacterial and antioxidant activities. *Heliyon* **2021**, *7*, e08459. [[CrossRef](#)]
40. Ibrahim, H.M.M. Green synthesis and characterization of silver nanoparticles using banana peel extract and their antimicrobial activity against representative microorganisms. *Radiat. Res. Appl. Sci.* **2015**, *8*, 265–476. [[CrossRef](#)]
41. Hoda, E.; Hamid, R.; Saeed, N. Synthesis and characterization of novel silver nanoparticles using *Chamaemelum nobile* extract for anti-bacterial application. *Adv. Nat. Sci. NanoSci. Nanotechnol.* **2017**, *8*, 025004.
42. Abbas, S.D. Biosynthesis of silver nanoparticles using lactobacillus and their effects on oxidative stress biomarkers in rats. *J. King Saud Univ. Sci.* **2017**, *29*, 462–467.
43. Prathibha, B.S.; Shanmuga Priya, K. Green synthesis of silver nanoparticles using *Tabebuia aurea* leaf extract. *IOSR J. Appl. Chem.* **2017**, *10*, 23–29. [[CrossRef](#)]
44. Elemike, E.E.; Onwudiwe, D.C.; Arijeh, O.; Nwankwo, H.U. Plant-mediated biosynthesis of silver nanoparticles by leaf extracts of *Lasienthra africanum* and a study of the influence of kinetic parameters. *Bull. Mater. Sci.* **2017**, *40*, 129–137. [[CrossRef](#)]
45. Somayeh, F.; Mina, J.; Mohammad, Y. Biologically synthesized silver nanoparticles by aqueous extract of *Satureja intermedia* C.A. Mey and the evaluation of total phenolic and flavonoid contents and antioxidant activity. *J. Nanostructure Chem.* **2016**, *6*, 357–364.
46. Gomathia, M.; Prakasama, A.; Rajkumar, P.V.; Rajeshkumar, S.; Chandrasekarand, R.; Anbarasan, P.M. Green synthesis of silver nanoparticles using *Gymnema sylvestre* leaf extract and evaluation of its anti-bacterial activity. *South Afr. J. Chem. Eng.* **2020**, *32*, 1–4. [[CrossRef](#)]
47. Wang, W.; Yu, Z.; Alsammarrarie, F.K.; Kong, F.; Lin, M.; Mustapha, A. Properties and antimicrobial activity of polyvinyl alcohol-modified bacterial nanocellulose packaging films incorporated with silver nanoparticles. *Food Hydrocoll.* **2021**, *100*, 105411. [[CrossRef](#)]
48. Akinuoye, A.G.; Salawu, Q.O.; James, O.G. Characterization of biosynthesized silver nanoparticles using UV-visible and FTIR Spectroscopy. *Afr. J. Environ. Sci. Technol.* **2020**, *3*, 21–26.
49. Huang, J.; Li, Q.; Sun, D.; Lu, Y.; SU, Y.; Yang, X.; Wang, H.; Wang, Y.; Shao, W.; He, N.; et al. Biosynthesis of silver and gold nanoparticles by novel sundried *Cinnamomum camphora* leaf. *Nanotechnology* **2007**, *18*, 105104. [[CrossRef](#)]
50. Sharifi-Rad, M.; Pohl, P.; Epifano, F.; Álvarez-Suarez, J.M. Green synthesis of silver nanoparticles using *Astragalus tribuloides* Delile. root extract: Characterization, antioxidant, anti-bacterial, and anti-inflammatory activities. *Nanomaterials* **2020**, *10*, 2383. [[CrossRef](#)]
51. Tahir, R.; Muhammad, B.; Iqbal, H.M.N.; Li, C. Green biosynthesis of silver nanoparticles using leaves extract of *Artemisia vulgaris* and their potential biomedical applications. *Colloids Surf. B Biointerfaces* **2017**, *158*, 408–415.
52. Vasudeo, K.; Priya, T. Biosynthesis of silver nanoparticles by using the Cinnamon (*Dalchini*) extract. *Curr. Pharma Res.* **2019**, *9*, 2716–2720.
53. Rajeswari, A.; Sujatha, D.; Balasaraswathi, K.; Mani, U.; Chellan, R.; Asit, B.M. Phytosynthesis of silver nanoparticles using *Coccinia grandis* leaf extract and its application in the photocatalytic degradation. *Colloids Surf. B Biointerfaces* **2012**, *94*, 226–230.
54. Rohan, S.P.; Anup, S.H. Sunlight induced green synthesis of silver nanoparticles using sundried leaves extract of *Kalanchoe pinnata* and evaluation of its photocatalytic potential. *Pharm. Lett.* **2015**, *7*, 313–324.
55. Mohanta, Y.K.; Panda, S.K.; Biswas, K.; Tamang, A.; Bandyopadhyay, J.; De, D.; Mohanta, D.; Bastia, A.K. Biogenic synthesis of silver nanoparticles from *Cassia fistula* (Linn.): In vitro assessment of their antioxidant, antimicrobial and cytotoxic activities. *IET Nanobiotechnol.* **2016**, *10*, 438–444. [[CrossRef](#)]
56. Abdel-Aziz, M.S.; Shaheen, M.S.; El-Nekeety, A.A.; Abdel-Wahhab, M.A. Antioxidant and anti-bacterial activity of silver nanoparticles biosynthesized using *Chenopodium murale* leaf extract. *J. Saudi Chem. Soc.* **2014**, *18*, 356–363. [[CrossRef](#)]

57. Fafal, T.; Taştan, P.; Tüzün, B.S.; Ozyazici, M.; Kivcak, B. Synthesis, characterization and studies on antioxidant activity of silver nanoparticles using *Asphodelus aestivus* Brot. aerial part extract. *S. Afr. J. Bot.* **2017**, *112*, 346–353. [[CrossRef](#)]
58. Dhanapal, A.C.T.A.; Warrant, A.N. Impact of *Ocimum tenuiflorum* mediated green synthesis of silver nanoparticles on in-vitro antioxidant and anti-bacterial activities. *Int. J. Pharm. Qual. Assur.* **2020**, *11*, 379–388. [[CrossRef](#)]
59. Nazarni, R.; Purnama, D.; Umar, S.; Eni, H. The effect of fermentation on total phenolic, flavonoid, and tannin content and its relation to anti-bacterial activity in Jaruk tigarun (*Crataeva nurvala*, Buch HAM). *Int. Food Res. J.* **2016**, *23*, 309–315.
60. Vorobyova, V.; Vasylyev, G.; Skiba, M. Eco friendly green synthesis of silver nanoparticles with the black currant pomace extract and its anti-bacterial, electrochemical, and antioxidant activity. *Appl. NanoSci.* **2020**, *10*, 4523–4534. [[CrossRef](#)]
61. Hussain, P.R.; Rather, S.A.; Suradkar, P.P. Structural characterization and evaluation of antioxidant, anticancer and hypoglycemic activity of radiation degraded oat (*Avena sativa*) β -glucan. *Radiat. Phys. Chem.* **2018**, *144*, 218–230. [[CrossRef](#)]
62. De Marco Castro, E.; Shannon, E.; Abu-Ghannam, N. Effect of fermentation on enhancing the nutraceutical properties of *Arthrospira platensis* (Spirulina). *Fermentation* **2019**, *5*, 28. [[CrossRef](#)]
63. Rabeta, M.S.; Lai, S.Y. Effects of drying, fermented and unfermented tea of *Ocimum tenuiflorum* Linn. on the antioxidant capacity. *Int. Food Res. J.* **2013**, *20*, 1601–1608.
64. Zangeneh, M.M.; Saneei, S.; Zangeneh, A. Preparation, characterization, and evaluation of cytotoxicity, antioxidant, cutaneous wound healing, anti-bacterial, and anti-fungal effects of gold nanoparticles using the aqueous extract of *Falcaria vulgaris* leaves. *Appl. Organomet. Chem.* **2019**, *33*, 5263. [[CrossRef](#)]
65. Netai, M.M.; Stephen, N.; Musekiwa, C. Synthesis of silver nanoparticles using wild *Cucumis anguria*: Characterization and anti-bacterial activity. *Afr. J. Biotechnol.* **2017**, *16*, 1911–1921.
66. Vidal, J.; Huiliñir, C.; Santander, R.; Silva-Agredo, J.; Torres-Palma, R.A.; Salazar, R. Degradation of ampicillin antibiotic by electrochemical processes: Evaluation of antimicrobial activity of treated water. *Environ. Sci. Pollut. Res.* **2019**, *26*, 4404–4414. [[CrossRef](#)] [[PubMed](#)]
67. Roy, A.; Bulut, O.; Some, S.; Mandal, A.K.; Yilmaz, M.D. Green synthesis of silver nanoparticles: Biomolecule-nanoparticle organisations targeting antimicrobial activity. *RSC Adv.* **2019**, *9*, 2673–2702. [[CrossRef](#)]
68. Siddiqui, M.N.; Redhwi, H.H.; Achilias, D.S.; Kosmidou, E.; Vakalopoulou, E.; Ioannidou, M.D. Green synthesis of silver nanoparticles and study of their antimicrobial properties. *J. Polym. Environ.* **2018**, *26*, 423–433. [[CrossRef](#)]
69. Ahmed, S.; Ahmad, M.; Swami, B.L.; Ikram, S. A review on plants extract mediated synthesis of silver nanoparticles for antimicrobial applications: A green expertise. *J. Adv. Res.* **2016**, *7*, 17–28. [[CrossRef](#)]
70. Salman, H.D. Evaluation and comparison the anti-bacterial activity of silver nano particles (AgNPs) and silver nitrate (AgNO₃) on some pathogenic bacteria. *J. Glob. Pharma Technol.* **2017**, *9*, 238–248.
71. Ocsy, I.; Demirbas, A.; McLamore, E.; Altinsoy, B.; Ildiz, N.; Baldemir, A. Green synthesis incorporated hydrothermal approaches for silver nanoparticles formation and enhanced antimicrobial activity against bacterial and fungal pathogens. *J. Mol. Liq.* **2017**, *238*, 263–269. [[CrossRef](#)]

Disclaimer/Publisher's Note: The statements, opinions and data contained in all publications are solely those of the individual author(s) and contributor(s) and not of MDPI and/or the editor(s). MDPI and/or the editor(s) disclaim responsibility for any injury to people or property resulting from any ideas, methods, instructions or products referred to in the content.